Rational Design of Amyloid Binding Agents Based on the Molecular Rotor Motif

Jeyanthy Sutharsan[a], **Marianna Dakanali**[a], **Christina C. Capule**[a], **Mark A. Haidekker**[b], **Jerry Yang**[a], and **Emmanuel A. Theodorakis**[a]

Jerry Yang: jerryyang@ucsd.edu; Emmanuel A. Theodorakis: etheodor@ucsd.edu

[a] Department of Chemistry and Biochemistry, University of California, San Diego, 9500 Gilman Drive, La Jolla, CA 92093-0358 (USA), Fax: (+1) 858-822-0386 (ET), Fax: (+1) 858-534-4554 (JY)

[b] Faculty of Engineering, University of Georgia, Athens, GA 30602 (USA)

Abstract

Alzheimer's disease (AD) is characterized by a progressive loss of cognitive function and constitutes the most common and fatal neurodegenerative disorder.[1] Genetic and clinical evidence supports the hypothesis that accumulation of amyloid deposits in the brain plays an important role in the pathology of the disease. This event is associated with perturbations of biological functions in the surrounding tissue leading to neuronal cell death, thus contributing to the disease process. The deposits are comprised primarily of amyloid (Aβ) peptides, a 39–43 amino acid sequence that self aggregates into a fibrillar β-pleated sheet motif. While the exact three-dimensional structure of the aggregated Aβ peptides is not known, a model structure that sustains the property of aggregation has been proposed.[2] This creates opportunities for in vivo imaging of amyloid deposits that can not only help evaluate the time course and evolution of the disease, but can also allow the timely monitoring of therapeutic treatments.[3]

Keywords

amyloid peptides; fluorescent probes; imaging agents; molecular rotors

Historically, Congo Red (CR) and Thioflavin T (ThT) have provided the starting point for the visualization of amyloid plaques and are still commonly employed in post mortem histological analyses (Figure 1).[4] However, due to their charge these probes are unsuitable for in vivo applications.[5] To address this issue, several laboratories developed probes with noncharged, lipophilic (log P = 0.1–3.5) and low-molecular weight chemical structures (MW <650) that facilitate crossing of the blood–brain barrier.[6] Further functionalization of these compounds with radionuclides led to a new generation of in vivo diagnostic reagents (Figure 1) that target plaques and related structures for imaging with positron emission tomography (PET) and single-photon emission computed tomography (SPECT).[7] Despite these advances, there is a pressing need for the design and development of new amyloid-targeting molecules with improved physical, chemical and biological characteristics.[8] At present, identification of new amyloid sensing molecules is based mainly on modification of existing dyes[9] and/or screening of libraries of dyes.[10]

Examination of the chemical structures shown in Figure 1 reveals that the majority of these probes contain an electrondonor unit in conjugation with an electron acceptor (D-π-A motif). This motif is a typical feature in molecular rotors, a family of fluorescent probes known to form twisted intramolecular charge-transfer (TICT) complexes in the excited state producing a fluorescence quantum yield that is dependent on the surrounding environment.[11] Following photoexcitation, this motif has the unique ability to relax either via fluorescence emission or via an internal nonradiative molecular rotation. This internal rotation occurs around the σ-bonds that connect the electron-rich π-system with the donor and acceptor groups, and can be modified by altering the chemical structure and microenvironment of the probe.[12] Hindrance of the internal molecular rotation of the probe by increasing the surrounding media rigidity, or by reducing the available free volume needed for relaxation, leads to a decrease in the nonradiative decay rate and consequently an increase in fluorescence. In contrast, relaxation proceeds mainly via nonradiative pathways in environments of low viscosity or of high free volume. Due to these properties, molecular rotors have been used to study polarity, free volume and viscosity changes in solvents and organized assemblies,[13] such as liposomes,[14] cells[15] and polymers.[16]

Intrigued by the above observations, we asked whether we could design amyloid-binding agents based on the molecular rotor motif. We envisioned that π-conjugation of a dialkyl amino group, as the electron donor (D), with a 2-cyano acrylate unit, as the electron acceptor (A), would produce Aβ-binding molecules with inherent fluorescence properties.[17] Interestingly, the fluorescence properties of such a motif could be fine-tuned by modifying the electronic density and extent of conjugation between the donor and acceptor units. The solubility of these amyloid-binding agents in aqueous media can be achieved by the introduction of water solubilizing groups (WSG), such as esters of triethylene glycol monomethyl ether (TEGME) or of glycerol. The design concept is shown in Figure 2.

Key to the synthesis of all probes was a Knoevenagel condensation of the appropriate aldehyde, for example, **6**, with the appropriate malonic acid derivative, for example, **7**, (Scheme 1). This reaction was catalyzed by piperidine and was completed within 21 h in refluxing THF.[18] After a standard chromatographic purification on silica gel, the desired product **8** was isolated in excellent yields (Table 1).

Naphthalene-based probe **11** was synthesized by treatment of commercially available methoxy naphthaldehyde **9** with lithiated piperidine[19] and Knoevenagel condensation of the resulting aldehyde **10** with cyano ester **7** (Scheme 2, 29 % combined yield).

Compound **14** was prepared by condensation of aldehyde **6 a** with α-cyano ester **12**, followed by an acid-catalyzed deprotection of the acetonide unit (Scheme 3, 68 % combined yield). [20]

Stilbene-based probe **19** was synthesized in four steps that included: a) conversion of benzyl bromide **15** to phosphonate **16**;[21]; b) Horner–Emmons olefination of **16** with aldehyde **6 a** to form **17**; c) lithiation of bromide **17** and formylation to produce aldehyde **18**; d) Knoevenagel condensation of the resulting aldehyde **18** with cyano ester **7** (Scheme 4, 42 % combined yield).

An initial study to determine whether a probe can associate with aggregated Aβ is to compare its fluorescence spectra before and after mixing with the Aβ aggregates.[9,10] Typically, a fluorescent amyloid-binding agent displays a significant fluorescence intensity increase after binding to Aβ aggregates as compared to its native fluorescence in solution.[22] Along these lines, we measured the fluorescent properties of each probe at 4 μM before and after mixing with preaggregated Aβ(1–42) peptides (5 μM, aggregated in PBS buffer for 3 days at 25 °C). In all cases, a 1.3- to 9.4-fold fluorescence intensity increase was observed in the presence of aggregated Aβ, indicating that these compounds bind to the peptide (Table 2). In most cases a

modest blue shift (6–20 nm) was observed upon binding. Only in the case of the naphthalene-based probe **11** was a significant red shift of 76 nm observed upon binding to preaggregated Aβ (Figure 3c and d). Interestingly, this binding was accompanied with a 9.3-fold intensity increase. A similar intensity increase has been observed with FDDNP[23] and may be explained by the ability of the naphthalene motif to create excimers upon binding to its target. [24] Probes **8 a** and **8b** exhibited similar fluorescence characteristics suggesting that addition of a methoxy group on the phenyl group does not alter the binding properties of the probe. On the other hand, it is worth noting that increasing the size of the alkyl groups of the nitrogen leads to a significant increase in the fluorescence intensity after binding (Table 2, **8 a**, **8c**, **8 d**). This is likely a result of the decreased rotational freedom of the molecules upon binding to the aggregated forms of Aβ peptide.[25] Interestingly, no increase of fluorescence intensity was observed upon mixing of these probes with monomeric Aβ peptide (see Supporting Information). This supports the notion that these probes bind selectively to aggregated forms of Aβ. The fluorescence profile of **8 d** (excitation and emission) is shown in Figure 3a and b.

We also measured the apparent binding constants (K_d) of the probes (in concentrations of 10, 5, 2.5 and 1.25 μM) to 5.0 μM pre-aggregated Aβ(1–42) peptide. The K_d can be measured from the double reciprocal of the fluorescence maximum (F_{max}) and the concentration of the probe. [22] All K_d values were measured between 1.4 and 5.3 μM (Table 2). It is remarkable that, despite the structural differences, these probes display similar K_d values suggesting that they bind in a similar fashion to aggregated Aβ. Moreover, these values are similar to the reported K_d values for ThT (2 μM).[22,26] The double reciprocal plot of fluorescence intensity versus concentration of probes **8 d** and **11** are shown in Figure 4. The K_d corresponds to the −1/(x-intercept) of the linear regression.[22]

The association of the synthesized compounds with aggregated Aβ peptides was tested using a semi-quantitative ELISA-based assay developed by Yang and co-workers.[27] The assay is based on screening for molecules that inhibit the interaction of the aggregated Aβ peptide with a monoclonal anti-Aβ IgG raised against residues 1–17 of Aβ. Table 2 shows the concentrations of the probes corresponding to 50 % inhibition (IC_{50}) of the IgG-Aβ interactions as well as the maximal percentage of IgG inhibited from binding to the aggregated peptide. All probes exhibited IC_{50} values at micromolar levels, the lowest value being measured for compound **8b** (IC_{50} = 1.2 μM). The maximum inhibition (I_{max}), a measure of the extent of surface coating of the aggregated peptide by the probes,[27] was determined to be between 40–98 % (Table 2). Comparison of these data indicates that the surface coating increases by decreasing the size of the probe or the extent of the π system. Specifically, while the maximum inhibition is between 81–98 % for the phenyl compounds, it decreases to 58 % for the longer naphthalene compound **11** and to 40 % for the more conjugated stilbene **19**. Representative graphs for **8 d** and **11** are shown in Figure 5.

The log P values for all the compounds were calculated to be between 1.07 and 4.62 (Table 2) [28] indicating that most of these probes meet the solubility criteria and should be able to cross the blood–brain barrier.[27,29] Finally, all compounds showed little or no cytotoxicity against human neuroblastoma cells at concentrations up to 100 μM (see Supporting Information). These properties represent significant advantages for further in vivo evaluation.

In conclusion, inspired by the structures of the currently used amyloid-binding agents we have evaluated the possibility to design new Aβ binding fluorescent probes based on the molecular rotor motif. We found that the molecular rotors, designed based on the concept shown in Figure 2, bind to the aggregated Aβ peptide with low micromolar affinity. We hypothesize that this binding is a result of hydrophobic interactions between the rotor and the amyloid peptide. This binding reduces the free volume around the rotor resulting in an increased fluorescence emission.[30] A similar effect has been reported for the binding of molecular rotors to actin,

albumin and other proteins.[31] We have demonstrated that these molecules can be readily synthesized and have no significant cytotoxicity. In addition, we have shown that both the physical properties and fluorescence profile of these probes can be fine tuned by modifying their chemical structure. Notably, substituent changes in the electron donor group can affect the intensity of fluorescence emission, while changes in the π-system can affect the emission wavelength. These effects can be implemented for the construction of multicolored dyes and can lead to potential applications for in vitro and in vivo imaging.[32] Interestingly, a recent report describes the identification of CRANAD-2,[33] a small molecule containing two electron-donating groups connected simultaneously via π-conjugation to a single difluoroboronate acceptor. This probe has a high affinity for Aβ aggregates (K_d = 38.0 nM) and suitable near-infrared fluorescence properties for in vivo imaging, further validating our proposed concept of exploring the molecular rotor motif for the development of new amyloid-imaging probes. These findings demonstrate that the D-π-A motif of molecular rotors, presented in Figure 2, is a privileged scaffold and represents an important first step for the rational design of new diagnostic tools for Alzheimer's disease and related amyloid-based neurodegenerative disorders.

Supplementary Material

Refer to Web version on PubMed Central for supplementary material.

Acknowledgments

References

1. a) Minati L, Edginton T, Bruzzone MG, Giaccone G. Am J Alzheimers Dis 2009;24:95–121. b) Schott JM, Kennedy J, Fox NC. Curr Opin Neurol 2006;19:552–558. [PubMed: 17102693]

2. a) Mathis CA, Wang Y, Klunk WE. Curr Pharm Des 2004;10:1469–1492. [PubMed: 15134570] b) Kim YS, Lee JH, Ryu J, Kim DJ. Curr Pharm Des 2009;15:637–658. [PubMed: 19199987]

3. a) Matthews B, Siemers ER, Mozley PD. Am J Geriatr Psychiatry 2003;11:146–159. [PubMed: 12611744] b) Nichols L, Pike VW, Cai LS, Innis RB. Biol Psychiatry 2006;59:940–947. [PubMed: 16487944] c) Golde TE, Bacskai BJ. Nat Biotechnol 2005;23:552–554. [PubMed: 15877070]

4. a) Kitts CC, Bout DAV. J Phys Chem B 2009;113:12090–12095. [PubMed: 19663402] b) Schmidt ML, Schuck T, Sheridan S, Kung MP, Kung H, Zhuang ZP, Bergeron C, Lamarche JS, Skovronsky D, Giasson BI, Lee VM, Trojanowski JQ. Am J Pathol 2001;159:937–943. [PubMed: 11549586]

5. Mathis CA, Bacskai BJ, Kajdasz ST, McLellan ME, Frosch MP, Hyman BT, Holt DP, Wang YM, Huang GF, Debnath ML, Klunk WE. Bioorg Med Chem Lett 2002;12:295–298. [PubMed: 11814781]

6. Ryu EK, Chen XY. Front Biosci 2008;13:777–789. [PubMed: 17981587]

7. a) Stephenson KA, Chandra R, Zhuang ZP, Hou C, Oya S, Kung MP, Kung HF. Bioconjugate Chem 2007;18:238–246. b) Nordberg A. Curr Opin Neurol 2007;17:398–402. [PubMed: 17620873] c) Garcia-Alloza M, Bacskai BJ. Neuro-Mol Med 2004;6:65–78.

8. a) Bacskai BJ, Klunk WE, Mathis CA, Hyman BT. J Cereb Blood Flow Metab 2002;22:1035–1041. [PubMed: 12218409] b) Burn DJ, O'Brien JT. Mov Disord 2003;18(Suppl 6):S88–95. [PubMed: 14502661]

9. a) Nesterov EE, Skoch J, Hyman BT, Klunk WE, Bacskai BJ, Swager TM. Angew Chem Int Ed 2005;44:5452–5456. b) Zhuang ZP, Kung MP, Kung HF. J Med Chem 2006;49:2841–2844. [PubMed: 16640346]

10. a) Li QA, Lee JS, Ha C, Park CB, Yang G, Gan WB, Chang YT. Angew Chem 2004;116:6491–6495.Angew Chem Int Ed 2004;43:6331–6335. b) Kung HF, Lee CW, Zhuang ZP, Kung MP, Hou C, Plossl K. J Am Chem Soc 2001;123:12740–12741. [PubMed: 11741464]

11. a) Grabowski ZR, Rotkiewicz K, Rettig W. Chem Rev 2003;103:3899–4031. [PubMed: 14531716] b) Haidekker MA, Theodorakis EA. Org Biomol Chem 2007;5:1669–1678. [PubMed: 17520133]

12. Loutfy RO. Pure Appl Chem 1986;58:1239–1248.

13. a) Viriot ML, Carré MC, Geoffroy-Chapotot C, Brembilla A, Muller S, Stoltz JF. Clin Hemorheol Microcirc 1998;19:151–160. [PubMed: 9849928] b) Haidekker MA, Brady TP, Lichlyter D, Theodorakis EA. Bioorg Chem 2005;33:415–425. [PubMed: 16182338]

14. Nipper ME, Majd S, Mayer M, Lee JCM, Theodorakis EA, Haidekker MA. Biochim Biophys Acta, Biomembr 2008;1778:1148–1153.

15. a) Haidekker MA, Ling TT, Anglo M, Stevens HY, Frangos JA, Theodorakis EA. Chem Biol 2001;8:123–131. [PubMed: 11251287] b) Haidekker MA, Tsai AG, Brady T, Stevens HY, Frangos JA, Theodorakis E, Intaglietta M. Am J Physiol Heart Circ Physiol 2002;282:1609–1614. c) Haidekker MA, Brady TP, Lichlyter D, Theodorakis EA. Bioorg Chem 2005;33:415–425. [PubMed: 16182338]

16. a) Frochot C, Muller C, Brembilla A, Carre MC, Lochon P, Viriot ML. Int J Polym Anal Charact 2000;6:109–122. b) Damas C, Adibnejad M, Benjelloun A, Brembilla A, Carre MC, Viriot ML, Lochon P. Colloid Polym Sci 1997;275:364–371.

17. a) Lord SJ, Conley NR, Lee HLD, Samuel R, Liu N, Twieg RJ, Moerner WE. J Am Chem Soc 2008;130:9204–9205. [PubMed: 18572940] b) Lord SJ, Conley NR, Lee HLD, Nishimura SY, Pomerantz AK, Willets KA, Lu ZK, Wang H, Liu N, Samuel R, Weber R, Semyonov A, He M, Twieg RJ, Moerner WE. ChemPhysChem 2009;10:55–65. [PubMed: 19025732]

18. a) Chen XH, Zhao ZJ, Liu Y, Lu P, Wang YG. Chem Lett 2008;37:570–571. b) Haidekker MA, Brady TP, Lichlyter D, Theodorakis EA. J Am Chem Soc 2006;128:398–399. [PubMed: 16402812]

19. Guo HM, Tanaka F. J Org Chem 2009;74:2417–2424. [PubMed: 19222210]

20. Haidekker MA, Brady TP, Chalian SH, Akers W, Lichlyter D, Theodorakis EA. Bioorg Chem 2004;32:274–289. [PubMed: 15210341]

21. a) Meier H, Karpuk E, Holst HC. Eur J Org Chem 2006:2609–2617. b) Viau L, Maury O, Le Bozec H. Tetrahedron Lett 2004;45:125–128.

22. LeVine H III. Protein Sci 1993;2:404–410. [PubMed: 8453378]

23. Agdeppa ED, Kepe V, Liu J, Flores-Torres S, Satyamurthy N, Petric A, Cole GM, Small GW, Huang SC, Barrio JR. J Neurosci 2001;21:189.

24. a) Abad S, Vaya I, Jimenez MC, Pischel U, Miranda MA. ChemPhysChem 2006;7:2175–2183. [PubMed: 16986198] b) Spies C, Gehrke R. J Phys Chem A 2002;106:5348–5352.

25. a) Schuddeboom W, Jonker SA, Warman JM, Leinhos U, Kuehnle W, Zachariasse KA. J Phys Chem 1992;96:10809–10819. b) Il'chev YV, Kühnle W, Zachariasse KA. J Phys Chem A 1998;102:5670–5680.

26. a) Lockhart A, Ye L, Judd DB, Merritt AT, Lowe PN, Morgenstern JL, Hong GZ, Gee AD, Brown J. J Biol Chem 2004;280:7677–7684. [PubMed: 15615711] b) Biancalana M, Makabe K, Koide A, Koide S. J Mol Biol 2008;383:205–213. [PubMed: 18762191] c) Biancalana M, Makabe K, Koide A, Koide S. J Mol Biol 2009;385:1052–1063. [PubMed: 19038267]

27. a) Inbar P, Yang J. Bioorg Med Chem Lett 2006;16:1076–1079. [PubMed: 16290147] b) Inbar P, Li CQ, Takayama SA, Bautista MR, Yang J. ChemBioChem 2006;7:1563–1566. [PubMed: 16927253] c) Inbar P, Bautista MR, Takayama SA, Yang J. Anal Chem 2008;80:3502–3506. [PubMed: 18380488]

28. Log *P* values were calculated using the Molinspiration Cheminformatics software. [Lastaccessed, November 20, 2010]. http://www.molinspiration.com/

29. Lipinski CA, Lombardo F, Dominy BW, Feeney PJ. Adv Drug Delivery Rev 1997;23:3–25.

30. a) Loutfy RO, Arnold BA. J Phys Chem 1982;86:4205–4211. b) Doolittle AK. J Appl Phys 1952;23:236–239.

31. a) Iio T, Takahashi S, Sawada S. J Biochem 1993;113:196–199. [PubMed: 8468324] b) Iwaki T, Torigoe C, Noji M, Nakanishi M. Biochemistry 1993;32:7589–7592. [PubMed: 8338855]

32. Sigurdson CJ, Peter K, Nilsson R, Hornemann S, Manco G, Polymenidou M, Schwarz P, Leclerc M, Hammarstrom P, Wuthrich K, Aguzzi A. Nat Methods 2007;4:1023–1030. [PubMed: 18026110]
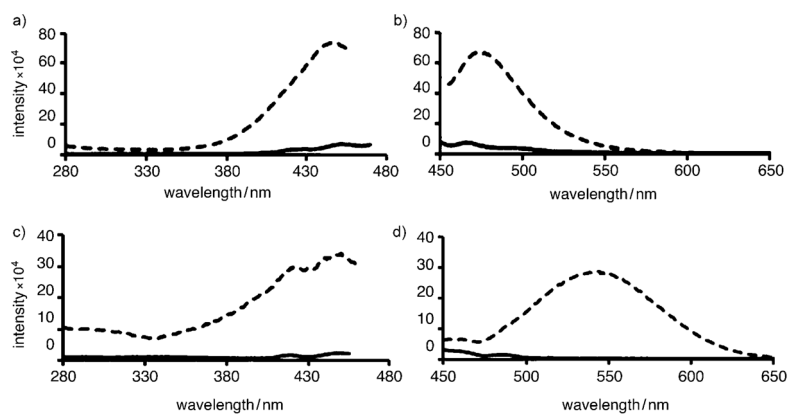
33. Ran C, Xu X, Raymond SB, Ferrara BJ, Neal K, Bacskai BJ, Medarova Z, Moore A. J Am Chem Soc 2009;131:15257–15261. [PubMed: 19807070]
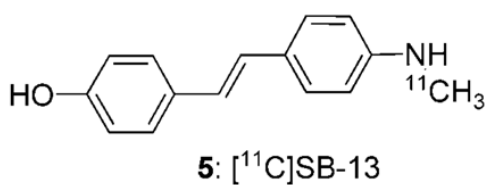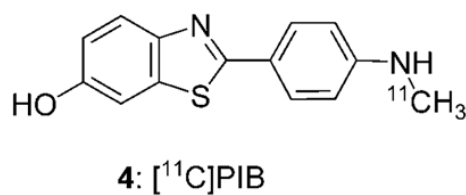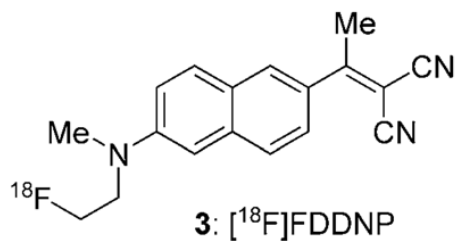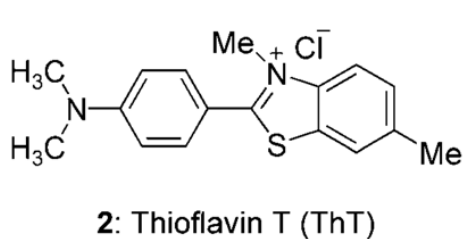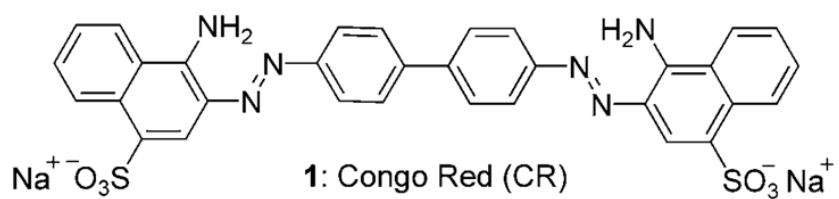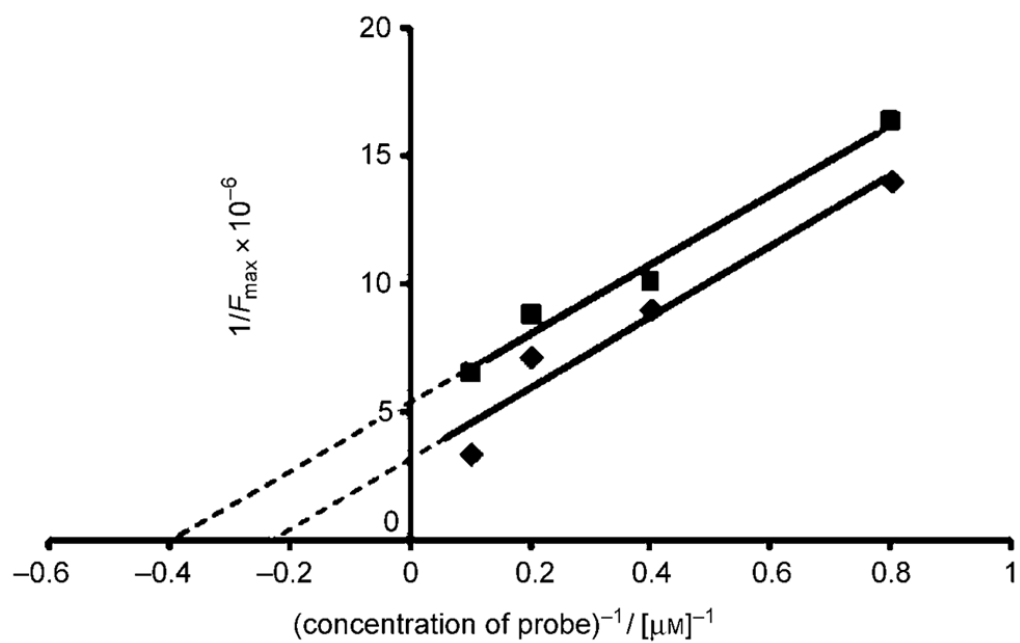
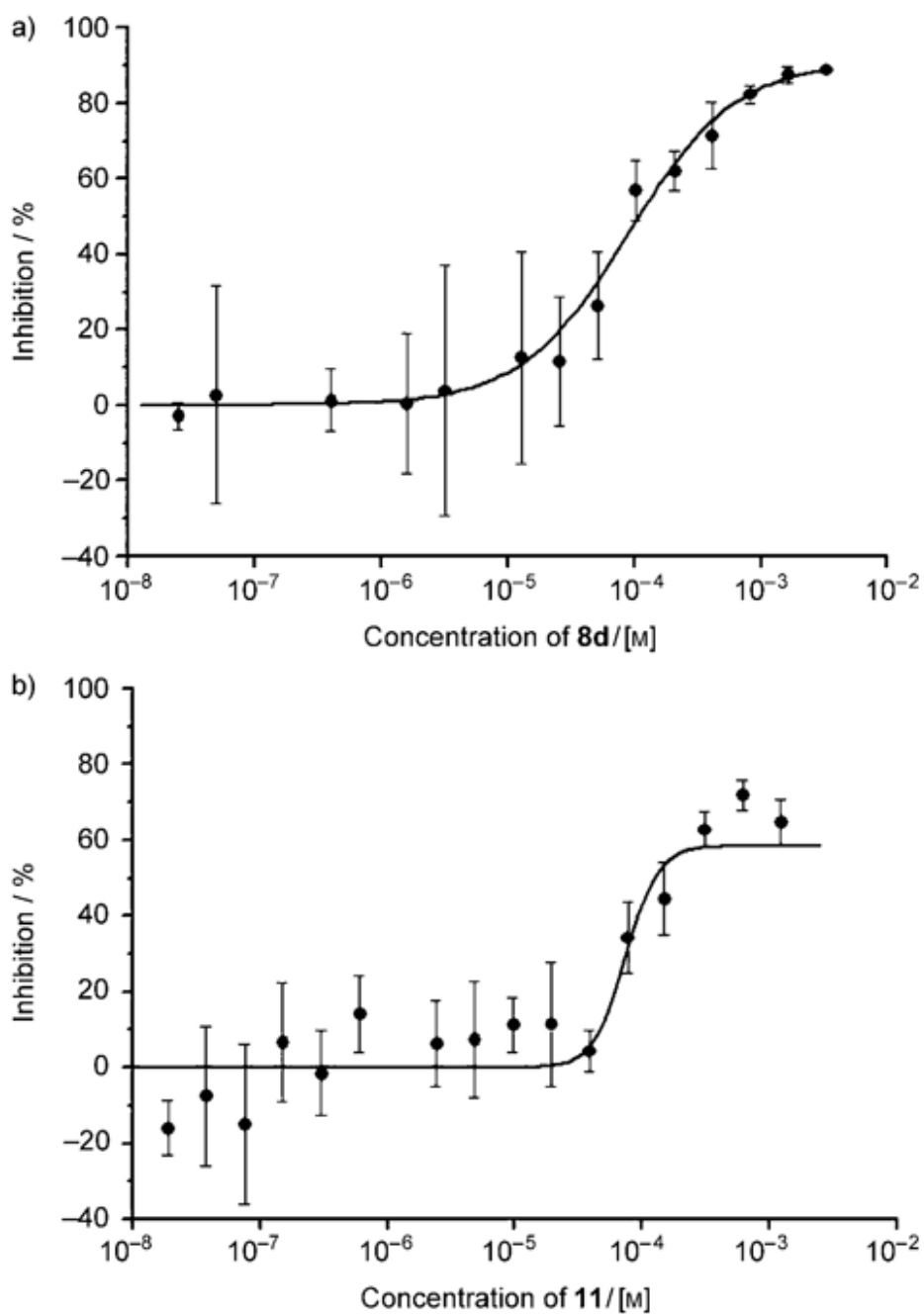**Figure 1.**
Structures of selected amyloid imaging reagents.
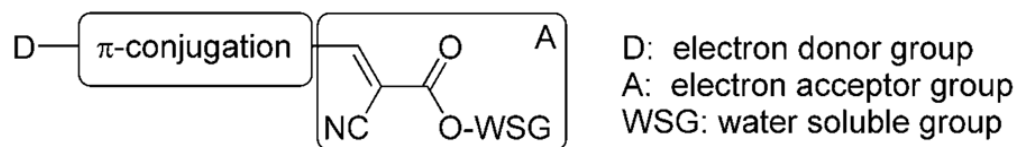
Figure 2.
Design of amyloid-binding agents based on the structure of a molecular rotor (D-π-A motif).

Figure 3.
Fluorescence excitation (a, c) and emission spectra (b, d) of probes **8d** (a, b) and **11** (c, d) in aqueous PBS solution (—) and in the presence of aggregated Aβ peptide (---).
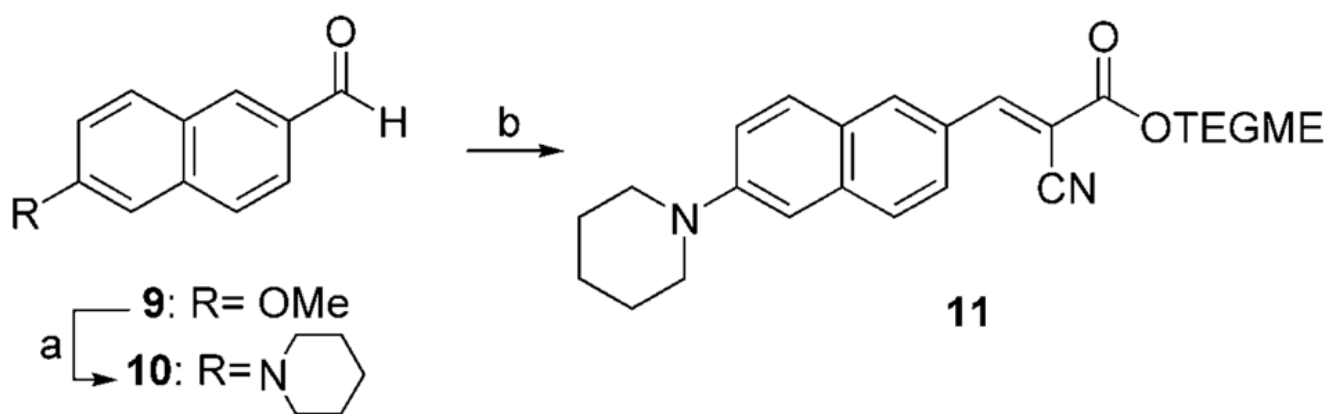
Figure 4.
Determination of the apparent binding constant (K_d) of probes **8d** ($\blacklozenge$; $R^2 = 0.95$) and **11** ($\blacksquare$; $R^2 = 0.98$) to preaggregated Aβ peptide.

Figure 5.
Inhibition of IgG-Aβ interactions with probes a) **8d** ($I_{max} = 91$ %, $IC_{50} = 91$ μM) and b) **11** ($I_{max} = 58$ %, $IC_{50} = 74$ μM).
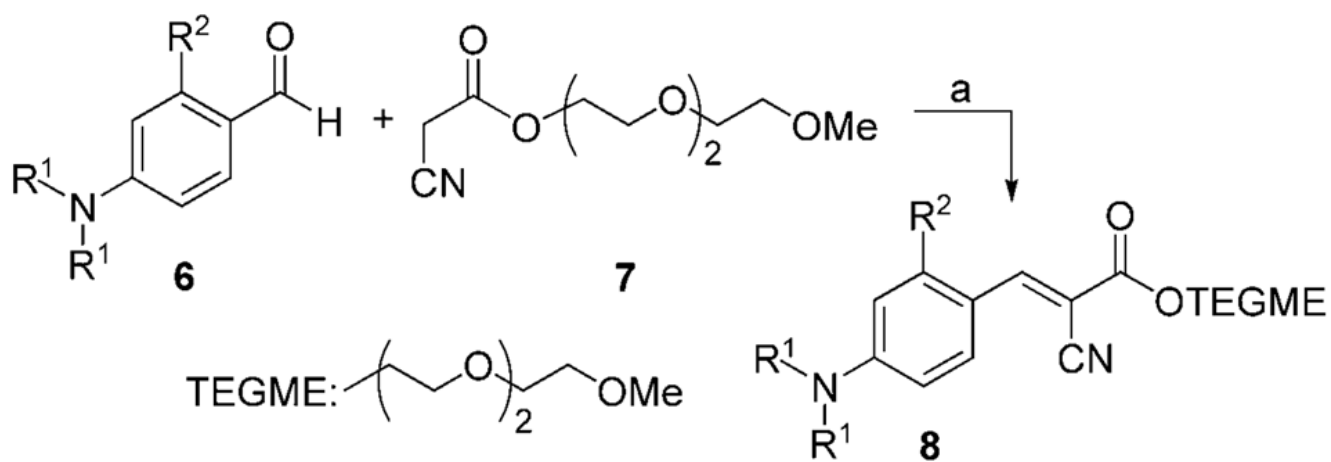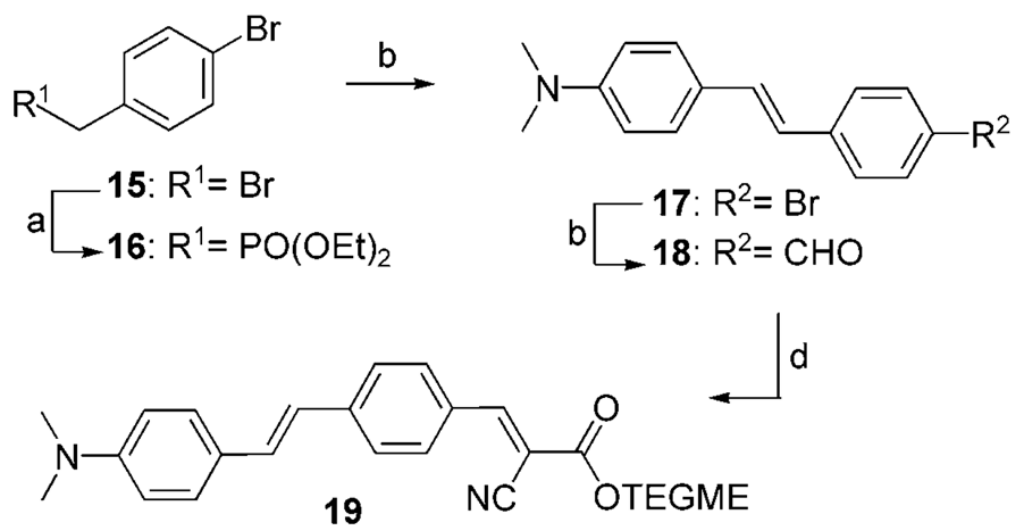
Scheme 1.
Reagents and conditions: a) 1.0 equiv **6**, 1.1 equiv **7**, 0.1 equiv piperidine, THF, 50 °C, 21 h.

Scheme 2.
Reagents and conditions: a) 8.0 equiv piperidine in benzene/HMPA: 1/1, 0 °C, 8.0 equiv *n*BuLi, 0 °C, 15 min, then 1.0 equiv **9**, 25 °C, 12 h, 35 %; b) 1.0 equiv **10**, 1.1 equiv **7**, 0.1 equiv piperidine, THF, 50 °C, 21 h, 82 %.
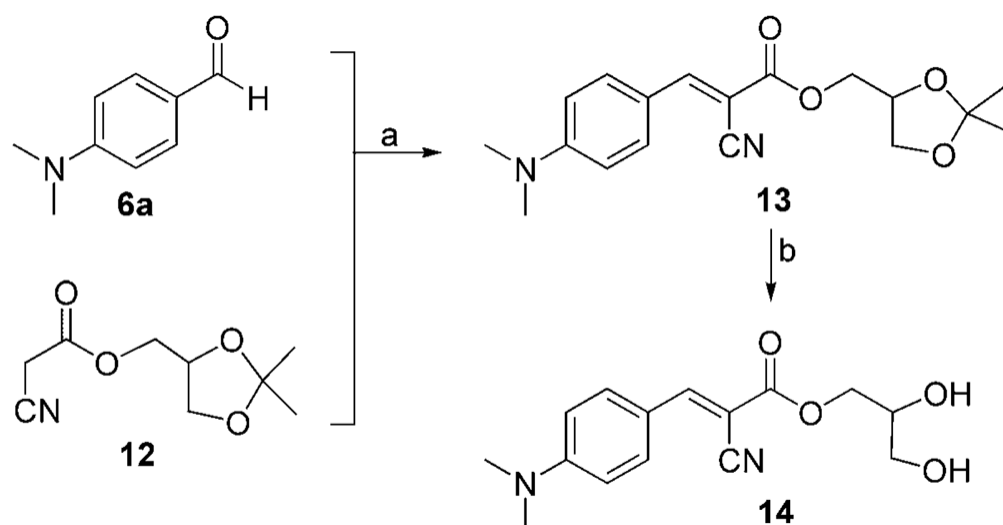
Scheme 3.
Reagents and conditions: a) 1.0 equiv **6a**, 1.1 equiv **12**, 0.1 equiv piperidine, THF, 50 °C, 21 h, 91 %; b) 1.5 mmol **13**, 0.10 g DOWEX-H$^+$, THF/CH$_3$OH (1:1), 25 °C, 20 h, 75 %.

Scheme 4.
Reagents and conditions: a) 1.0 equiv **15**, 15 equiv triethyl phosphite, 90 °C, 19 h, 98 %; b)
1.0 equiv **16**, 1.0 equiv NaOMe, 1.0 equiv **6a**, excess DMF, 25 °C, 24 h, 74 %; c) 1.0 equiv
17, 1.0 equiv *n*BuLi, 1.33 equiv DMF, THF, −78 °C, 60 %; d) 1.0 equiv **18**, 1.1 equiv **7**, 0.1
equiv piperidine, THF, 50 °C, 21 h, 97 %.

Table 1

Structures and yields of probes **8a–8d.**

Compd	R¹	R²	Yield (%)
8a	Me	H	98
8b	Me	OMe	98
8c	Et	H	90
8d	*n*Bu	H	78

Table 2

Fluorescence profile, K_d, IC_{50} and related values for the interaction of the synthesized probes with aggregated Aβ(1–42) peptides.

Compd	Excitation Maximum[a] [nm]		Emission Maximum[a] [nm]		Fold increase	K_d [μM]	R^2	I_{max}^b [%]	IC_{50}^b [μM]	Log P
	before	after	before	after						
8a	439	435	476	470	1.8	2.6	0.93	81	129.0	1.74
8b	442	444	478	469	1.3	5.3	0.99	92	1.2	1.54
8c	445	442	478	470	4.2	4.8	0.96	98	11.4	2.49
8d	432	440	466	468	9.4	4.4	0.95	91	90.6	4.62
11	445	440	462	538	9.3	2.5	0.98	58	74.3	3.81
14	437	434	476	467	2.2	3.3	0.99	79	82.1	1.07
19	312	319	658	638	2.3	1.4	0.98	40	33.6	4.30

[a]Before or after binding.

[b]Maximum percent inhibition (I_{max}) and IC_{50} values were determined by ELISA assay.